

Z.A. Gulshan, M.Z.H. Ali, M.S. Shah, D. Nouman, M. Anwar, M.F. Ullah

## A ROBUST CONTROL DESIGN APPROACH FOR ALTITUDE CONTROL AND TRAJECTORY TRACKING OF A QUADROTOR

**Introduction.** Unmanned aerial vehicles as quadcopters, twin rotors, fixed-wing crafts, and helicopters are being used in many applications these days. Control approaches applied on the quadrotor after decoupling the model or separate altitude control and trajectory tracking have been reported in the literature. A robust linear  $H_\infty$  controller has been designed for both altitude control and circular trajectory tracking at the desired altitude. **Problem.** The ability of the quadrotor system to hover at a certain height and track any desired trajectory makes their use in many industrial applications in both military and civil applications. Once a controller has been designed, it may not be able to maintain the desired performance in practical scenarios, i.e. in presence of wind gusts. **Originality.** This work presents the control strategy to ensure both altitude control and trajectory tracking using a single controller. **Purpose.** However, there is a need for a single controller that ensures both altitude control and trajectory tracking. **Novelty.** This paper presents a robust  $H_\infty$  control for altitude control and trajectory tracking for a six degree of freedom of unmanned aerial vehicles quadrotor. **Methodology.** Multi input multi output robust  $H_\infty$  controller has been proposed for the quadrotor for altitude control and tracking the desired reference. For the controller validation, a simulation environment is developed in which a 3D trajectory is tracked by the proposed control methodology. **Results.** Simulation results depict that the controller is efficient enough to achieve the desired objective at minimal control efforts. **Practical value.** To verify that the proposed approach is able to ensure stability, altitude control, and trajectory tracking under practical situations, the performance of the proposed control is tested in presence of wind gusts. The ability of the controller to cater to the disturbances within fractions of seconds and maintaining both transient and steady-state performance proves the effectiveness of the controller. References 16, table 1, figures 9.

**Key words:**  $H_\infty$  controller, six degree of freedom quadrotor, unmanned aerial vehicle, attitude regulation, nonlinear system, robust control.

**Вступ.** Безпілотні літальні апарати, такі як квадрокоптери, двороторні апарати, апарати з нерухомими крилами та гелікоптери сьогодні використовуються у багатьох сферах застосування. У літературі повідомляється про підходи до керування, застосовані на квадрокоптері після від'єднання моделі або окремого контролю висоти та відстеження траєкторії. Надійний лінійний регулятор  $H_\infty$  був розроблений як для контролю висоти, так і для відстеження кругової траєкторії на потрібній висоті. **Проблема.** Здатність квадрокоптерної системи зависати на певній висоті та відстежувати будь-яку бажану траєкторію робить їх застосування можливим у багатьох сферах як у військових, так і в цивільних цілях. Розроблений контролер може не підтримувати бажані характеристики у реальних умовах, тобто за наявності поривів вітру. **Оригінальність.** У цій роботі представлена стратегія керування, яка забезпечує як контроль висоти, так і відстеження траєкторії за допомогою одного контролера. **Мета.** Однак існує потреба в єдиному контролері, який забезпечує як контроль висоти, так і відстеження траєкторії. **Новизна.** У цій статті представлено надійний регулятор  $H_\infty$  для контролю висоти та відстеження траєкторії для шести ступенів свободи безпілотних літальних апаратів. **Методологія.** Для квадрокоптера запропоновано багатовхідний багатовихідний надійний контролер  $H_\infty$  для контролю висоти та відстеження бажаного курсу. Для перевірки контролера розробляється середовище моделювання, в якому тривимірна траєкторія відстежується за запропонованою методологією керування. **Результати.** Результати моделювання показують, що контролер є досить ефективним для досягнення бажаної мети при мінімальних зусиллях контролю. **Практична цінність.** Щоб переконатися, що запропонований підхід здатний забезпечити стабільність, контроль висоти та відстеження траєкторії в реальних ситуаціях, параметри запропонованого контролю перевіряються за наявності поривів вітру. Здатність контролера усувати порушення протягом кількох секунд і підтримувати як перехідні, так і стабільні показники доводить ефективність контролера. Бібл. 16, табл. 1, рис. 9.

**Ключові слова:**  $H_\infty$  контролер, квадрокоптер з шістьма ступенями свободи, безпілотний літальний апарат, регулювання позиції, нелінійна система, надійне керування.

**1. Introduction.** Unmanned Aerial Vehicles (UAV) like fixed wing crafts, quadcopters, and helicopters have found applications in several domains [1]. Amongst these, quadcopters and helicopters are commonly used as UAVs due to their hovering ability. These systems possess nonlinear and coupled dynamics, which leads to the challenges in their autonomous control. The dynamics of helicopter can be approximated by a laboratory setup namely Twin Rotor Aerodynamic System (TRAS) [2]. Like helicopter, TRAS has two rotors main and tail rotors. Though in helicopter, main rotor is able to tilt in order to execute forward motion [3].

Control design for UAVs is a difficult task because of the coupling and nonlinearities involved in their mathematical models. In autonomous applications, trajectory tracking is one of the most basic and important tasks. Other equally important scenarios involve e.g.,

hover control. In [4], four independent proportional–integral–derivative (PID) controllers with independent inputs for control have been designed to achieve the objective of trajectory tracking. Here, real value type genetic algorithm has been used to tune the controller parameters in order to reduce total error and control efficiency. System performance index is used as a fitness function here. In [5], hover control problem is addressed by a control structure that involves feedback and feed forward control. Four impulse input shaper is used for feed forward and PID controller with acceleration feedback input is used for the tracking controller. In [6], robust PID based dead beat control scheme is proposed. As PID controller does not contain the model information, so for small dynamic systems, it performs reasonably well but for higher order system it may lead to oscillations. To

© Z.A. Gulshan, M.Z.H. Ali, M.S. Shah, D. Nouman, M. Anwar, M.F. Ullah

counter these problems, different model-based controllers have been reported in the literature. In [7] an linear-quadratic regulator (LQR) controller is designed. In [8], an integral sliding mode controller using necessary and sufficient conditions has been proposed for the uncertainty handling and trajectory tracking of the quadrotor. A nonlinear PID control strategy is discussed in [9] for the trajectory tracking of the quadrotor. The method proposed here is a novel contribution of nonlinearity in the conventional PID controller based on frequency domain design. A model free control approach is used in [10] for the quadrotor trajectory tracking. Control structure adopted here is based on the internal-external-control-loop structure. Controller uses the conventional sliding mode approach for control effort generation. A super twisting slide mode approach has been used in [11] for trajectory tracking with the nonlinear sliding surface. Experimental validation of the proposed control architecture has also been included. A neural network based self-tuning control structure using double derivative action with proportional control is proposed in [12] for trajectory tracking of the quadrotor UAV. Fractional slide mode control is also proposed for the quadrotor in [13].

The single-input single-output (SISO) linear time invariant (LTI) controllers like proportional-derivative (PD), proportional-integral (PI) and PID require the decoupling of the multi-input multi-output (MIMO) model of the quadrotor which takes the extra computational effort, i.e. one needs to design a de-coupler to obtain multiple SISO models from a single MIMO model of the quadrotor and then design the SISO controller for each model. This may also cause slowing the closed-loop response of the system when connected with hardware and thus can be resulted in an increased control effort and poor tracking. However, the MIMO LTI controllers like LQR, Linear Quadratic Gaussian (LQG), and  $H_\infty$  controllers tend to have a larger control effort while trajectory tracking for a quadrotor.

Nonlinear controllers on the other hand require that the desired trajectory be twice differentiable, i.e. 1<sup>st</sup> and 2<sup>nd</sup> derivatives of the reference trajectory are required to design the nonlinear controller like slide mode, flatness based, backstepping, twisted slide mode and twisted backstepping controllers. Thus, in case of a fast-changing input trajectory, i.e. reference trajectory with the sharp edges, the value of its 1<sup>st</sup> and 2<sup>nd</sup> derivatives become sufficiently high leading to the instability of the closed-loop system. So, the controller designed using these approaches ensures the trajectory tracking only for the smooth reference trajectories and hence the tracking of a circular trajectory, even in 3D is possible with these nonlinear approaches is possible. But the trajectories with sharp edges, i.e. square and triangular trajectories can't be tracked. Also, the nonlinear controller based the system dynamics has the equal computational complexity to that of its nonlinear model and thus for the high nonlinear and more complex system like quadrotor, the computational complexity is increased which may cause slowing the closed-loop response when connected to the hardware for experiments. While the nonlinear controller designed through heuristic and intuitional approaches like neural

network and fuzzy logic, one needs to have the complete information and knowledge about the system behavior and design the set of rules to design a controller ensuring the desired performance. One drawback of using these approaches is once the designer misinterprets the system behavior, intentionally or unintentionally, the resulting controller will lead the instability of the closed system. So, one need to have complete information about the system and consider all the ambiguities, disturbances in each operating zone, and understand the system performance under every possible condition. This requires a lot of experience and experimentation.

**Aim and objectives of the paper.** Motivated by the issue mentioned above a single multi-input multi-output linear time invariant controller has been designed that can ensure both altitude control and trajectory tracking in presence of wind gusts and measurement noise. The main contribution of this work is design of a single robust controller for flight control of the quadrotor, i.e. make it fly to achieve a certain altitude and then track the desired trajectory.

Following objectives are met to reach the stated aim of the research:

- a MIMO  $H_\infty$  controller design for the quadrotor model;
- application of designed controller in feedback with the quadrotor model for altitude control and trajectory tracking;
- introduction of wind gusts and measurement noise to verify the controller performance.

Rest of the paper is organized as follows: Section 2 describes the control oriented mathematical modeling of quadrotor. Section 3 briefly discusses the control design approach proposed in the paper. Discussion on the simulation results are presented in Section 4 and, finally, conclusions are drawn in Section 5.

**2. Mathematical modeling of the quadrotor.** Quadrotor consists of four arms bearing equal weights and length with a DC motor embedded in each of them to achieve the desired motion in a three-dimensional space. The inertial reference frame of a quadrotor system can be seen in Fig. 1.

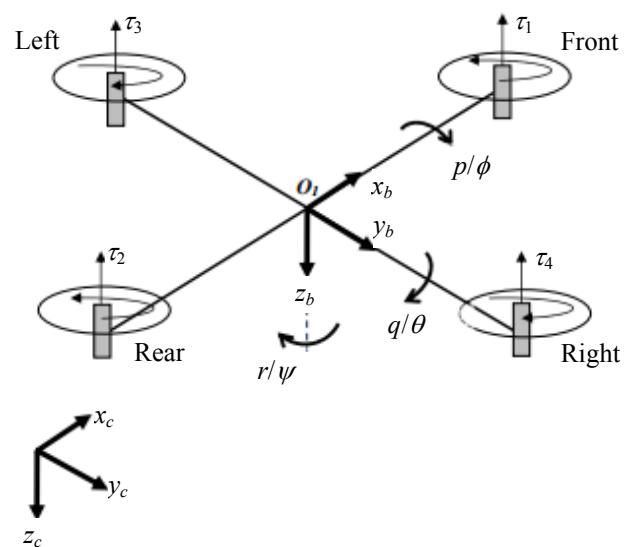


Fig. 1. Inertial reference frame of a quadrotor

Rotor angular positions of the motors can be denoted by  $\Omega_i$  where  $i$  represents the motor on the  $i^{\text{th}}$  arm of the quadrotor and  $i = 1, 2, 3, 4$ . The angular velocities are denoted by  $\omega_i$ . Rear and front rotors of the quadrotor revolve in counter-clock-wise-direction by angular speeds  $\omega_1$  and  $\omega_2$ , thus generate the thruster torques  $\tau_2$  and  $\tau_1$  respectively. While motors 2 and 3 rotate in clock-wise-direction generating torques  $\tau_3$  and  $\tau_4$ .

For hovering the quadrotor at a specific height, clock- and counter clock-wise-torques are desired to be the same and thus rotating the respective motors at a same speed, i.e. balancing the body weight of the quadrotor, is the main concern. Since the motor operate as to generate the thruster torques in opposite direction, there is no imbalance of the quadrotor reaction torque, i.e. there is zero imbalance in reaction torque. Roll, pitch and yaw angles, while considering the angular positions of the quadrotor body, are denoted by  $\phi$ ,  $\theta$  and  $\psi$  respectively. Roll angle is created by increasing (decreasing) the speed of motor associated with right propeller and decreasing (increasing) that of the left one to make the body roll or turn along its own axis.

Throttle is achieved by rotating all the motors (propellers) in same direction at a same speed. Pitch angle is associated with the angular speed of front and rear motors and yaw movement can be generated by moving the front-rear and left-right propellers. If the speed of one pair, described earlier, is increasing that of the other should be reducing to generate the yaw movement. Three orthogonal movements in space and same number of orthogonal movements of the quadrotor offer six degree-of-freedom (DOF). The state-space of the quadrotor is given in (1). For the detailed study of the mathematical model, reader is referred to [14].

$$\begin{bmatrix} \phi \\ \ddot{\theta} \\ \ddot{\psi} \\ \ddot{x} \\ \ddot{y} \\ \ddot{z} \end{bmatrix} = \begin{bmatrix} 1 & 0 & 0 & 0 & 0 & 0 \\ 0 & 1 & 0 & 0 & 0 & 0 \\ 0 & 0 & 1 & 0 & 0 & 0 \\ 0 & 0 & 0 & A_x & 0 & 0 \\ 0 & 0 & 0 & 0 & A_y & 0 \\ 0 & 0 & 0 & 0 & 0 & A_z \end{bmatrix} \cdot \begin{bmatrix} \dot{\phi} \\ \dot{\theta} \\ \dot{\psi} \\ \dot{x} \\ \dot{y} \\ \dot{z} \end{bmatrix} - \begin{bmatrix} 0 \\ 0 \\ 0 \\ 0 \\ 0 \\ -g \end{bmatrix} + \begin{bmatrix} 0 \\ 0 \\ 0 \\ 0 \\ 0 \\ 1 \end{bmatrix} \cdot \frac{F}{m}. \quad (1)$$

Equation (1) represents the state-space model of the 6-DOF quadrotor. However, the detailed state-space model can be represented by the state-space equations given in (2)-(13) [14]

$$\dot{x}_1 = x_2; \quad (2)$$

$$\dot{x}_2 = \frac{l \cdot k (\omega_4^2 - \omega_2^2)}{I_{xx}}; \quad (3)$$

$$\dot{x}_3 = x_4; \quad (4)$$

$$\dot{x}_4 = \frac{l \cdot k (\omega_3^2 - \omega_1^2)}{I_{yy}}; \quad (5)$$

$$\dot{x}_5 = x_6; \quad (6)$$

$$\dot{x}_6 = \frac{b (\omega_1^2 - \omega_2^2 + \omega_3^2 - \omega_4^2)}{I_{zz}}; \quad (7)$$

$$\dot{x}_7 = x_8; \quad (8)$$

$$\dot{x}_8 = A_x x_1; \quad (9)$$

$$\dot{x}_9 = x_{10}; \quad (10)$$

$$\dot{x}_{10} = A_y x_3; \quad (11)$$

$$\dot{x}_{11} = x_{12}; \quad (12)$$

$$\dot{x}_{12} = A_z x_5 - g + \frac{1}{m} (\omega_1^2 + \omega_2^2 + \omega_3^2 + \omega_4^2); \quad (13)$$

where  $\omega_i$  represent the angular velocities of the motor on  $i^{\text{th}}$  arm of the quadrotor;  $g$  is the gravitational acceleration;  $l$ ,  $b$ ,  $k$ ,  $m$  denote the arm length, coefficient of left and right drag, and mass of the quadrotor respectively;  $I_{xx}$ ,  $I_{yy}$  and  $I_{zz}$  denote the moments of inertia in  $x$ ,  $y$  and  $z$  axis respectively.

The set of state equations written in (2) – (13) are converted into state-space. The state-space matrices of the system are written as follows:

$$A = \begin{bmatrix} 0 & 1 & 0 & 0 & 0 & 0 & 0 & 0 & 0 & 0 & 0 & 0 & 0 \\ 0 & 0 & 0 & 0 & 0 & 0 & 0 & 0 & 0 & 0 & 0 & 0 & 0 \\ 0 & 0 & 0 & 0 & 0 & 0 & 0 & 0 & 0 & 0 & 0 & 0 & 0 \\ 0 & 0 & 0 & 1 & 0 & 0 & 0 & 0 & 0 & 0 & 0 & 0 & 0 \\ 0 & 0 & 0 & 0 & 0 & 1 & 0 & 0 & 0 & 0 & 0 & 0 & 0 \\ 0 & 0 & 0 & 0 & 0 & 0 & 0 & 0 & 0 & 0 & 0 & 0 & 0 \\ 0 & 0 & 0 & 0 & 0 & 0 & 0 & 0 & 1 & 0 & 0 & 0 & 0 \\ 0 & 0 & 0 & 0 & 0 & 0 & 0 & 0 & 0 & 0 & 0 & 0 & 0 \\ A_x & 0 & 0 & 0 & 0 & 0 & 0 & 0 & 0 & 0 & 0 & 0 & 0 \\ 0 & 0 & 0 & 0 & 0 & 0 & 0 & 0 & 0 & 0 & 1 & 0 & 0 \\ 0 & 0 & A_y & 0 & 0 & 0 & 0 & 0 & 0 & 0 & 0 & 0 & 0 \\ 0 & 0 & 0 & 0 & 0 & 0 & 0 & 0 & 0 & 0 & 0 & 0 & 1 \\ 0 & 0 & 0 & 0 & A_z & 0 & 0 & 0 & 0 & 0 & 0 & 0 & 0 \end{bmatrix}; \quad (14)$$

$$B = \begin{bmatrix} 0 & 0 & 0 & 0 \\ 0 & -l \cdot k / I_{xx} & 0 & l \cdot k / I_{xx} \\ 0 & 0 & 0 & 0 \\ -l \cdot k / I_{yy} & 0 & l \cdot k / I_{yy} & 0 \\ 0 & 0 & 0 & 0 \\ b / I_{zz} & -b / I_{zz} & b / I_{zz} & -b / I_{zz} \\ 0 & 0 & 0 & 0 \\ 0 & 0 & 0 & 0 \\ 0 & 0 & 0 & 0 \\ 0 & 0 & 0 & 0 \\ k & k & k & k \end{bmatrix}; \quad (15)$$

$$C = \begin{bmatrix} 1 & 0 & 0 & 0 & 0 & 0 & 0 & 0 & 0 & 0 & 0 & 0 & 0 \\ 0 & 0 & 1 & 0 & 0 & 0 & 0 & 0 & 0 & 0 & 0 & 0 & 0 \\ 0 & 0 & 0 & 0 & 1 & 0 & 0 & 0 & 0 & 0 & 0 & 0 & 0 \\ 0 & 0 & 0 & 0 & 0 & 0 & 1 & 0 & 0 & 0 & 0 & 0 & 0 \\ 0 & 0 & 0 & 0 & 0 & 0 & 0 & 0 & 1 & 0 & 0 & 0 & 0 \\ 0 & 0 & 0 & 0 & 0 & 0 & 0 & 0 & 0 & 0 & 1 & 0 & 0 \end{bmatrix}. \quad (16)$$

The inputs, states, and outputs of the systems are given in (17)–(19), respectively

$$u = [\omega_1^2 \ \omega_2^2 \ \omega_3^2 \ \omega_4^2]^T; \quad (17)$$

$$x = [\phi \ \dot{\phi} \ \theta \ \dot{\theta} \ \psi \ \dot{\psi} \ x \ \dot{x} \ y \ \dot{y} \ z \ \dot{z}]^T; \quad (18)$$

$$y = [\phi \ \theta \ \psi \ x \ y \ z]^T. \quad (19)$$

The angular positions of the motors at quadrotor arms can be given as

$$\Omega_i = \frac{K_m \cdot r_a \cdot \eta \cdot N}{J} \cdot V_i, \quad (20)$$

where  $V_i$  is the input voltage for the  $i^{\text{th}}$  motor and  $\omega_i = \dot{\Omega}_i$ , rest of the parameters and their corresponding values are given in Table 1.

Table 1

Parameters of the quadrotor

Parameter	Value	Parameter	Value
$A_x$	0,45	$I_{xx}$ , kg·m <sup>2</sup>	0,357·10 <sup>-5</sup>
$A_y$		$I_{yy}$ , kg·m <sup>2</sup>	
$A_z$		$I_{zz}$ , kg·m <sup>2</sup>	
$k$	2,98·10 <sup>-6</sup>	$m$ , kg	1,316
$g$ , m/s <sup>2</sup>	9,8	$l$ , m	0,5

This model of the quadrotor is used to design the robust  $H_\infty$  controller for the flight control. A brief discussion about the controller design is given in the following section.

**3. Robust control design.** Controller is placed with the system for controlling the plant according to desired parameters and responses. Main objective general configuration of plant  $P$  (to be controlled) with the controller  $K$  is shown in Fig. 2.

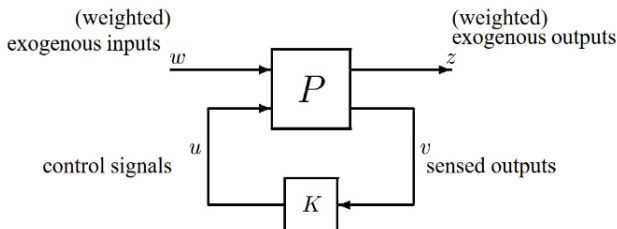


Fig. 2. General plant with controller configuration

Objective is to minimize the norm of transfer function from  $w$  to  $z$  and the design problem is to find controller gain  $K$  based on  $v$  which gives  $u$  as control signal to the plant which minimize the closed loop norm from  $w$  to  $z$ . The generalized configuration will then be represented as [15]:

$$\begin{bmatrix} z \\ v \end{bmatrix} = P(s) \begin{bmatrix} w \\ u \end{bmatrix} = \begin{bmatrix} P_{11}(s) & P_{12}(s) \\ P_{21}(s) & P_{22}(s) \end{bmatrix} \begin{bmatrix} w \\ u \end{bmatrix}; \quad (21)$$

$$u = K(s) \cdot v. \quad (22)$$

The linear fractional transformation is

$$z = F_l(P, K)w, \quad (23)$$

where

$$F_l(P, K) = P_{11} + P_{12}K(1 - P_{22}K)^{-1}P_{21}. \quad (24)$$

### 3.1. $H_\infty$ controller.

The  $H_\infty$  optimal control problem is to find all stabilizing controllers  $K$  that minimize [15]

$$\|F_l(P, K)\|_\infty = \max_w \bar{\sigma}(F_l(P, K) \cdot (j\omega)). \quad (25)$$

The  $H_\infty$  norm has several interpretations in terms of performance. One is that it minimizes the peak of the maximum singular value of  $F_l(P(j\omega), K(j\omega))$ . In practice, it is usually not necessary to obtain an optimal controller for the  $H_\infty$  problem, and it is often computationally (and theoretically) simpler to design a suboptimal one (i.e. one close to the optimal ones in the sense of the  $H_\infty$  norm). Let  $\gamma_{\min}$  be the minimum value of overall stabilizing controllers  $K$ . Then the  $H_\infty$  sub-optimal control problem is: given a  $\gamma > \gamma_{\min}$ , find all stabilizing controllers  $K$  such that

$$\|F_l(P, K)\|_\infty = \gamma. \quad (26)$$

If we desire a controller that achieves  $\gamma_{\min}$ , to within a specified tolerance, then we can perform a bisection on  $\gamma$  until its value is sufficiently accurate. The above result provides a test for each value of  $\gamma$  to determine whether it is less than  $\gamma_{\min}$  or greater than  $\gamma_{\min}$ .

Two methods are there for  $H_\infty$  controller design: the transfer function shaping approach and the signal-based approach. In the former,  $H_\infty$  optimization is used to shape the singular values of specified transfer functions over frequency. The maximum singular values are relatively easy to shape by forcing them to lie below user defined bounds, thereby ensuring desirable widths and roll-off rates. In the signal-based approach, we seek to minimize the energy in certain error signals given a set of exogenous input signals [16]. The latter might include the outputs of perturbations representing uncertainty, as well as the usual disturbances, noise, and command signals. Both two approaches will be considered again in the remainder of this section. In each case we will examine a problem and formulate it in the general control configuration.

A difficulty that sometimes arises with  $H_\infty$  control is the selection of weights such that the  $H_\infty$  optimal controller provides a good trade-off between conflicting objectives in various frequency ranges. Thus, for practical designs it is sometimes recommended to perform only a few iterations of the  $H_\infty$  algorithm. The justification for this is that the initial design, after one iteration, is like a  $H_2$  design which does trade-off over various frequency ranges. Therefore, stopping the iterations before the optimal value is achieved gives the design  $H_2$  flavor which may be desirable.

**4. Results and discussions.** For the controller validation, a simulation environment is developed in which a 3D trajectory is tracked by the proposed control methodology.

Figures 3, 4 show the tracking of  $x$  and  $y$  coordinates. It can be observed from plots that controller reaches and stay on desired  $x$  and  $y$  coordinates with minimum estimation error.

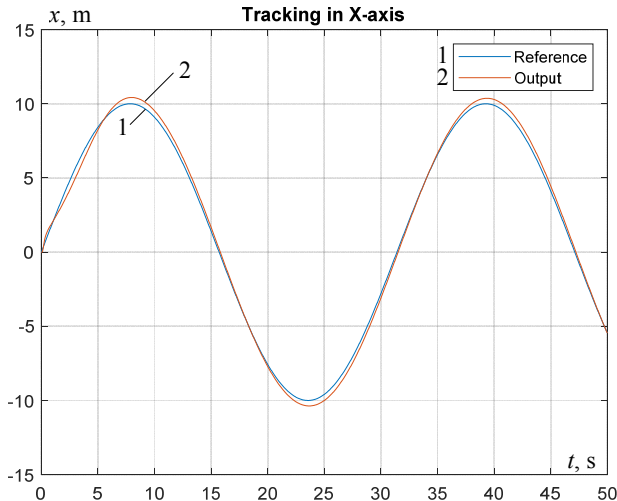


Fig. 3. Tracking of  $x$  coordinates

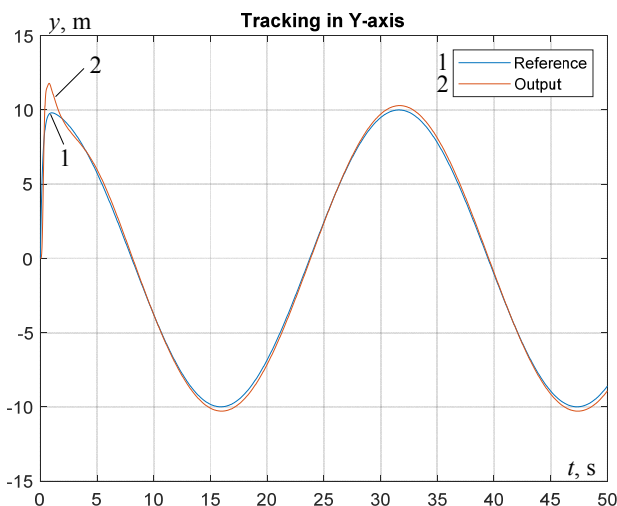


Fig. 4. Tracking of  $y$  coordinates

Initially it is assumed that, quadrotor is hovering at zero altitude. Then it is desired that it gains 10 m of height with slowly increasing altitude value as shown in Fig. 5.

After gaining the desired height it is aimed that quadrotor moves in a circular trajectory having radius of 10 m as shown in the Fig. 5. From Fig. 5, 6, it can be observed that initially tracking error is high but few seconds later controller achieves the desired height. Quadrotor reaches desired altitude within 5 s, which is reasonable performance. After gaining desired altitude quadrotor tracks the specified trajectory with minimum estimation error. From Fig. 5, the tracking of circular trajectory can be seen. Despite the tracking of desired trajectory, the most important is that quadrotor maintains its stable attitudes. Stability of attitudes mean that quadrotor do not observe the excessive roll and pitch

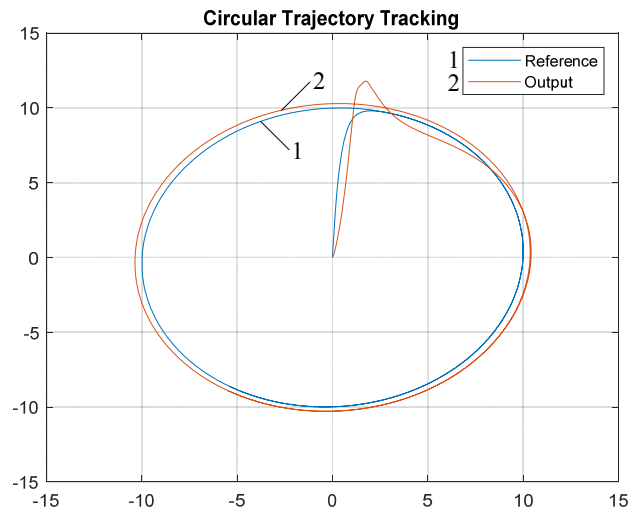


Fig. 5. Tracking of planar trajectory

motion. If quadrotor tracks the desired trajectory under excessive roll and pitch motion, then stability of motion cannot be guaranteed. Actually, it is the best possible case that quadrotor tracks the desired trajectory with minimum roll and pitch angle.

The tracking of desired attitude is displayed in Fig. 6, the plot shows that initially at starting point quadrotor start motion with greater pitch and roll angle but after 1 s of flight it achieves attitudes close to zero. These observation increases the confidence on controller performance and real time implication of designed control scheme. At last the most important observation is the control efforts calculated by controller. In existing case the control efforts are the angular velocities of four motors.

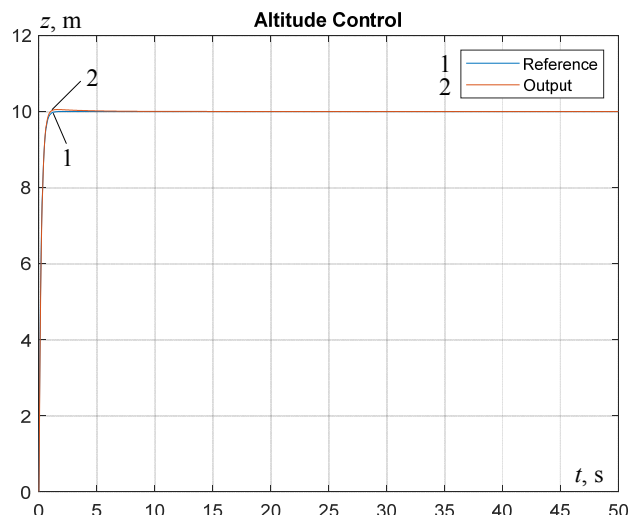


Fig. 6. Tracking of desired altitude

Figures 7–9 show the control effort plots. From the plots it can be seen that controller calculates smooth control inputs for motors with no chattering. Initially large fluctuations in motor speed can be seen but after 2 s they gains the steady value that are consistent with the trajectory tracking and attitude tracking of the quadrotor.

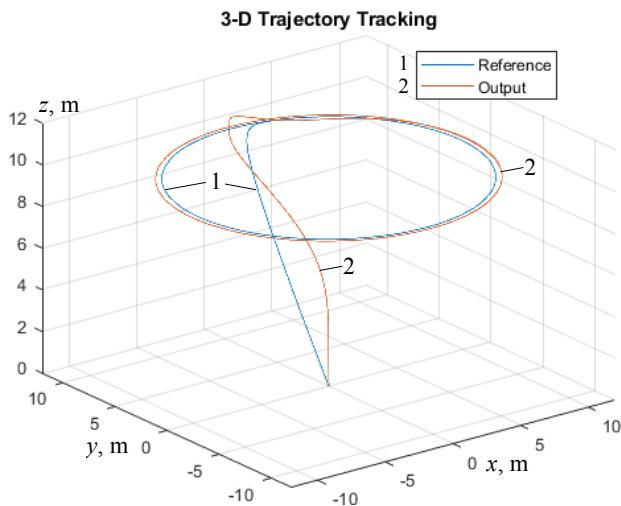


Fig. 7. Tracking of 3D trajectory

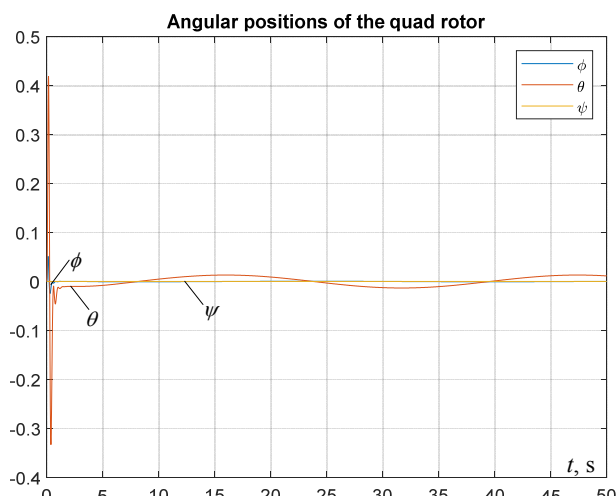


Fig. 8. Attitudes of quadrotor

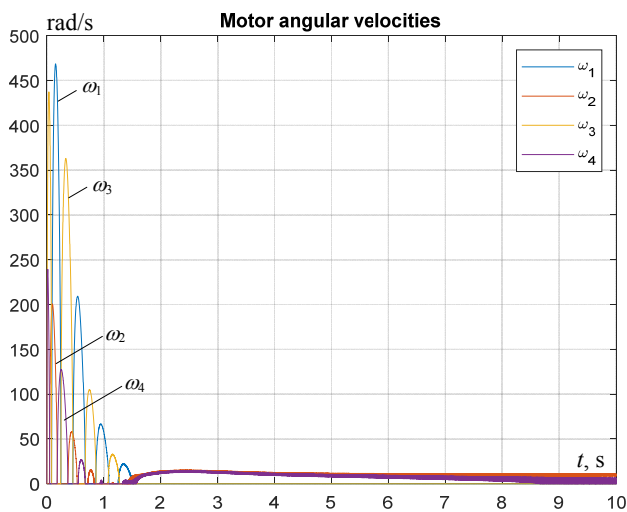


Fig. 9. Quadrotor motor speeds

## 5. Conclusions.

A robust  $H_\infty$  single Multi input multi output linear time invariant controller for six degree of freedom quadrotor has been designed that can ensure both altitude control and trajectory tracking in presence of wind gusts and measurement noise. Quadrotor is first lifted to the height of 10 m and after achieving the desired altitude, it

starts moving in circular path which keeping roll and pitch angles at  $0^\circ$ . Roll, pitch and angles are shown in results and discussion section. From the plots it can be seen that controller calculates smooth control inputs for motors with no chattering. Initially large fluctuations in motor speed can be seen but after 2 s they gains the steady value that are consistent with the trajectory tracking and attitude tracking of the quadrotor. In future, same work can be applied to the quadrotor by considering the wind gusts.

**Conflict of interest.** The authors declare that they have no conflicts of interest.

## REFERENCES

1. Valavanis K.P., Vachtsevanos G.J. *Handbook of unmanned aerial vehicles*. Springer Science + Business Media Dordrecht, 2015. doi: <https://doi.org/10.1007/978-90-481-9707-1>.
2. Luzar M., Korbicz J. Linear parameter-varying two rotor aero-dynamical system modelling with state-space neural network. In: Rutkowski L., Scherer R., Korytkowski M., Pedrycz W., Tadeusiewicz R., Zurada J. (eds) *Artificial Intelligence and Soft Computing, ICAISC 2018. Lecture Notes in Computer Science*, 2018, vol. 10842. Springer, Cham. doi: [https://doi.org/10.1007/978-3-319-91262-2\\_52](https://doi.org/10.1007/978-3-319-91262-2_52).
3. Venkatesan C. *Fundamentals of helicopter dynamics*. CRC Press, 2014. 338 p. doi: <https://doi.org/10.1201/b17314>.
4. Juang J., Huang M., Liu W. PID control using presearched genetic algorithms for a MIMO system. *IEEE Transactions on Systems, Man, and Cybernetics, Part C (Applications and Reviews)*, 2008, vol. 38, no. 5, pp. 716-727. doi: <https://doi.org/10.1109/tsmcc.2008.923890>.
5. Aldebrez F.M., Alam M.S., Tokhi M.O. Input-shaping with GA-tuned PID for target tracking and vibration reduction. *Proceedings of the 2005 IEEE International Symposium on, Mediterrean Conference on Control and Automation Intelligent Control*, 2005, pp. 485-490, doi: <https://doi.org/10.1109/2005.1467063>.
6. Wen P., Lu T.W. 2008. Decoupling control of a twin rotor MIMO system using robust deadbeat control technique. *IET Control Theory & Applications*, 2008, vol. 2, no. 11, pp. 999-1007. doi: <http://dx.doi.org/10.1049/iet-cta:20070335>.
7. Pratap B., Agrawal A., Purwar S. Optimal control of twin rotor MIMO system using output feedback. *2012 2nd International Conference on Power, Control and Embedded Systems*, 2012, pp. 1-6. doi: <https://doi.org/10.1109/icpces.2012.6508113>.
8. Thien R.T.Y., Kim Y. Decentralized formation flight via PID and integral sliding mode control. *Aerospace Science and Technology*, 2018, vol. 81, pp. 322-332. doi: <https://doi.org/10.1016/j.ast.2018.08.011>.
9. Moreno-Valenzuela J., Pérez-Alcocer R., Guerrero-Medina M., Dzul A. Nonlinear PID-type controller for quadrotor trajectory tracking. *IEEE/ASME Transactions on Mechatronics*, 2018, vol. 23, no. 5, pp. 2436-2447. doi: <https://doi.org/10.1109/TMECH.2018.2855161>.
10. Li, Z., Ma, X. and Li, Y., 2018. Model-free control of a quadrotor using adaptive proportional derivative-sliding mode control and robust integral of the signum of the error. *International Journal of Advanced Robotic Systems*, 15(5), p.1729881418800885. doi: <https://doi.org/10.1177/1729881418800885>.
11. Li Z., Ma X., Li Y. Model-free control of a quadrotor using adaptive proportional derivative-sliding mode control and robust integral of the signum of the error. *International Journal of Advanced Robotic Systems*, 2018, vol. 15, no. 5, p. 1729881418800888. doi: <https://doi.org/10.1177/1729881418800885>.
12. Tran T.-T., Ha C. Self-tuning proportional double derivative-like neural network controller for a quadrotor.

*International Journal of Aeronautical and Space Sciences*, 2018, vol. 19, no. 4, pp. 976-985. doi: <https://doi.org/10.1007/s42405-018-0091-6>.

13. Govea-Vargas A., Castro-Linares R., Duarte-Mermoud M., Aguila-Camacho N., Ceballos-Benavides G. Fractional order sliding mode control of a class of second order perturbed nonlinear systems: application to the trajectory tracking of a quadrotor. *Algorithms*, 2018, vol. 11, no. 11, p. 168. doi: <https://doi.org/10.3390/a11110168>.

14. Tengis T., Batmunkh A. State feedback control simulation of quadcopter model. *2016 11th International Forum on Strategic Technology (IFOST)*, 2016, pp. 553-557. doi: <https://doi.org/10.1109/ifost.2016.7884178>.

15. Skogestad S., Postlethwaite I. *Multivariable feedback control: analysis and design*. New York, Wiley, 2005.

16. John L., Mija S.J. Robust  $H_\infty$  control algorithm for Twin Rotor MIMO System. *2014 IEEE International Conference on Advanced Communications, Control and Computing Technologies*, 2014, pp. 168-173. doi: <https://doi.org/10.1109/ICACCCT.2014.7019402>.

Zulfiqar Ali Gulshan<sup>1</sup>, Engineer, MS,  
Muhammad Zulqarnain Haider Ali<sup>2</sup>, Engineer, MS,  
Muhammad Shahzaib Shah<sup>2</sup>, Engineer, MS,  
Danish Nouman<sup>2</sup>, Engineer, MS,  
Mehwish Anwar<sup>2</sup>, Engineer, MS,  
Mian Farhan Ullah<sup>3</sup>, Engineer, Lecturer,

<sup>1</sup> Department of Electrical Engineering,  
Fast University CHT-FSD campus,  
CHT-FSD, Islamabad, Pakistan,  
e-mail: gulshan037@gmail.com

<sup>2</sup> Department of Electrical Engineering,  
University of Engineering and Technology, Taxila, Pakistan,  
e-mail: mzulqarnain.haider@students.uettaxila.edu.pk;  
m.shahzaibshah@students.uettaxila.edu.pk;  
danishnouman1@gmail.com;  
mehwishanwar4455@gmail.com;

<sup>3</sup> Department of Electrical Engineering,  
Wah Engineering College, University of Wah,  
Quaid Avenue, Wah Cantt, Rawalpindi District,  
Punjab 47040, Pakistan.

e-mail: farhan.ullah@wecuw.edu.pk (Corresponding author)

Received 13.06.2021

Accepted 28.08.2021

Published 26.10.2021